

Supporting information:

$\text{Cp}_2\text{Ni}^{[1]}$ and $[\text{CpNi}(\text{COD})]\text{BF}_4^{[2]}$ were both synthesized according to literature procedures. DIB ligands were synthesised by sonication of the corresponding aniline with 2,3-butadione.

Synthesis of 1. A solution of $[\text{Ni}(\text{cp})(\text{cod})]\text{BF}_4$ (100 mg (0.314 mmol)) and Ph-DAB_{Me} (74 mg (0.314 mmol)) in dry THF (25 mL) were refluxed under Argon atmosphere for one hour. After the solution turned dark pink the solvent was removed and the solid recrystallized with DCM/ *n*-Hexane. Red crystals were obtained. Yield: 112 mg; 80%. Anal. Calc. for $\text{C}_{21}\text{H}_{21}\text{N}_2\text{NiBF}_4$ (found): C, 56.44 (55.65), H, 4.74 (4.72), N, 6.27 (6.15). ^1H NMR (250 MHz, CD_2Cl_2) δ [ppm]: 7.35 (dt, J = 28.0, 7.3 Hz, 6H), 7.06 (d, J = 7.4 Hz, 4H), 4.97 (s, 5H), 2.07 (s, 6H). ESI-MS: ($\text{C}_{21}\text{H}_{21}\text{N}_2\text{Ni}$) m/z 359.11

Synthesis of 2. A solution of $[\text{Ni}(\text{cp})(\text{cod})]\text{BF}_4$ (100 mg (0.314 mmol)) and 2-CF₃Ph-DAB_{Me} (116 mg (0.314 mmol)) in dry THF (25 mL) were refluxed under Argon atmosphere for one hour. After the solution turned dark purple the solvent was removed and the solid recrystallized with DCM/ *n*-Hexane. Purple crystals were obtained. Yield: 165 mg; 90%. Anal. Calc. for $\text{C}_{23}\text{H}_{19}\text{BF}_{10}\text{N}_2\text{Ni}$ (found): C, 47.39 (47.64), H, 3.29 (3.54), N, 4.81 (5.04). ^1H NMR (250 MHz, CDCl_3) δ [ppm]: 7.73 (m, 6H), 7.47 (t, J = 7.5 Hz, 2H), 4.95 (s, 5H), 2.10 (s, 6H). **MS:** m/z : ($\text{C}_{23}\text{H}_{19}\text{F}_6\text{N}_2\text{Ni}^+$): 495.08

Synthesis of 3. A solution of $[\text{Ni}(\text{cp})(\text{cod})]\text{BF}_4$ (100 mg (0.314 mmol)) and 2-OMePh-DAB_{Me} (93 mg (0.314 mmol)) in dry THF (25 mL) were refluxed under Argon atmosphere for one hour. After the solution turned dark red, the solvent was removed and the solid recrystallized with DCM/ *n*-Hexane. Red crystals were obtained. Yield: 151 mg; 95%. Anal. Calc. for $\text{C}_{23}\text{H}_{25}\text{BF}_4\text{N}_2\text{NiO}_2$ (found) C, 54.44 (54.42), H, 4.97 (5.01), N, 5.53 (5.61); ^1H NMR (250 MHz, CD_2Cl_2) δ [ppm]: 7.38 (t, J = 6.7 Hz, 2H), 7.10 (dd, J = 18.2, 7.6 Hz, 6H), 5.00 (s, 5H), 3.95 (s, 6H), 2.05 (s, 6H). ESI-MS: m/z : ($\text{C}_{23}\text{H}_{25}\text{N}_2\text{NiO}_2^+$) 419.13

[1] W. L. Jolly, D. J. Chazan, N. A. D. Carey, H. C. Clark, in *Inorganic Syntheses*, John Wiley & Sons, Inc., **2007**, pp. 122-123.

[2] A. Salzer, T. L. Court, H. Werner, *J. Organomet. Chem.* **1973**, 54, 325-330.

Table 1 Crystal data and structure refinement for of [CpNiL]BF₄

| Identification code | ac353_[CpNi(dab)]BF ₄ | ac352_[CpNi(dabf)]BF ₄ | ac354_[CpNi(dabome)]BF ₄ |
|--|---|--|--|
| Empirical formula | C ₂₁ H ₂₁ BN ₂ F ₄ Ni | C ₂₃ H ₁₉ BN ₂ F ₁₀ Ni | C ₂₃ H ₂₅ BN ₂ O ₂ F ₄ Ni |
| Formula weight | 446.93 | 582.11 | 506.47 |
| Temperature/K | 100.02 | 99.99 | 100 |
| Crystal system | orthorhombic | orthorhombic | monoclinic |
| Space group | Pnma | Pca2 ₁ | Cc |
| a/Å | 11.9844(8) | 19.7420(17) | 9.1415(8) |
| b/Å | 15.3276(11) | 7.5757(5) | 21.906(2) |
| c/Å | 10.8448(8) | 15.8268(13) | 11.8206(10) |
| $\alpha/^\circ$ | 90 | 90 | 90 |
| $\beta/^\circ$ | 90 | 90 | 104.863(4) |
| $\gamma/^\circ$ | 90 | 90 | 90 |
| Volume/Å ³ | 1992.1(2) | 2367.0(3) | 2287.9(4) |
| Z | 4 | 4 | 4 |
| $\rho_{\text{calc}}/\text{g cm}^{-3}$ | 1.49 | 1.6333 | 1.4702 |
| μ/mm^{-1} | 1.019 | 0.913 | 0.903 |
| F(000) | 921.9 | 1176.8 | 1048.8 |
| Crystal size/mm ³ | 0.594 × 0.194 × 0.167 | 0.209 × 0.188 × 0.116 | 0.322 × 0.198 × 0.105 |
| Radiation | Mo K α (λ = 0.71073) | Mo K α (λ = 0.71073) | Mo K α (λ = 0.71073) |
| 2 θ range for data collection/ $^\circ$ | 4.6 to 52.94 | 4.12 to 52.78 | 3.72 to 52.88 |
| Index ranges | -15 ≤ h ≤ 15, -13 ≤ k ≤ 19, -12 ≤ l ≤ 13 | -23 ≤ h ≤ 24, -9 ≤ k ≤ 6, -19 ≤ l ≤ 17 | -11 ≤ h ≤ 11, -26 ≤ k ≤ 27, -14 ≤ l ≤ 14 |
| Reflections collected | 24840 | 16211 | 15856 |
| Independent reflections | 2133 [R _{int} = 0.0312, R _{sigma} = 0.0160] | 4737 [R _{int} = 0.0703, R _{sigma} = 0.0946] | 4550 [R _{int} = 0.0312, R _{sigma} = 0.0498] |
| Data/restraints/parameters | 2133/90/139 | 4737/21/336 | 4550/108/334 |
| Goodness-of-fit on F ² | 1.067 | 1.008 | 1.036 |
| Final R indexes [I > 2 σ (I)] | R ₁ = 0.0311, wR ₂ = 0.1099 | R ₁ = 0.0473, wR ₂ = 0.0778 | R ₁ = 0.0552, wR ₂ = 0.1373 |
| Final R indexes [all data] | R ₁ = 0.0431, wR ₂ = 0.1290 | R ₁ = 0.0834, wR ₂ = 0.0892 | R ₁ = 0.0673, wR ₂ = 0.1453 |
| Largest diff. peak/hole / e Å ⁻³ | 0.69/-0.60 | 0.76/-0.70 | 0.55/-0.42 |
| Flack parameter | | -0.00(2) | 8.539(15) |

| Bond | 1 ⁺ | 2 ⁺ | 3 ⁺ | Free Ligand (Ph){Kovach, 2011 #236} | Free Ligand (o- CF3){Bomfim, 2007 #235} | Free Ligand (o- Me) |
|--------|----------------|----------------|----------------|---|--|---------------------------|
| Ni1–N1 | 1.8544(16) | 1.870(3) | 1.866(4) | | | |
| Ni1–N2 | 1.8544(16) | 1.867(3) | 1.881(6) | | | |
| Ni1–Cp | 1.699 | 1.714 | 1.718 | | | |
| N1–C6 | 1.307(3) | 1.301(5) | 1.319(6) | 1.281 | 1.280 | 1.280(2) |
| N2–C7 | 1.307(3) | 1.317(5) | 1.304(7) | 1.281 | 1.280 | 1.280(2) |
| C6–C7 | 1.465(4) | 1.472(6) | 1.461(7) | 1.503 | 1.513 | 1.502(2) |

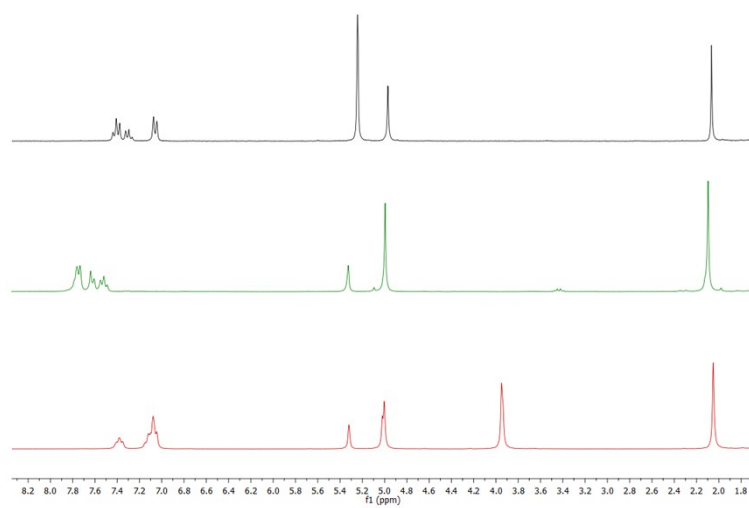


Figure S1. ^1H -NMR of complexes 1^+ , 2^+ , and 3^+ in CD_2Cl_2

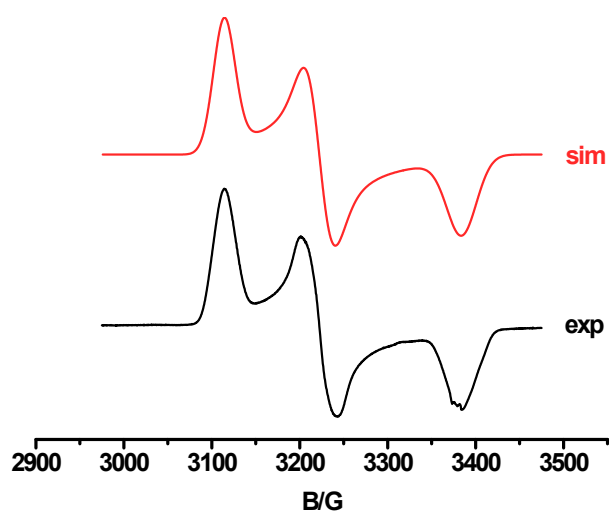


Figure S2. ESR Spectrum of the chemically reduced species 1^+ with Cp_2Co in toluene, 120 K

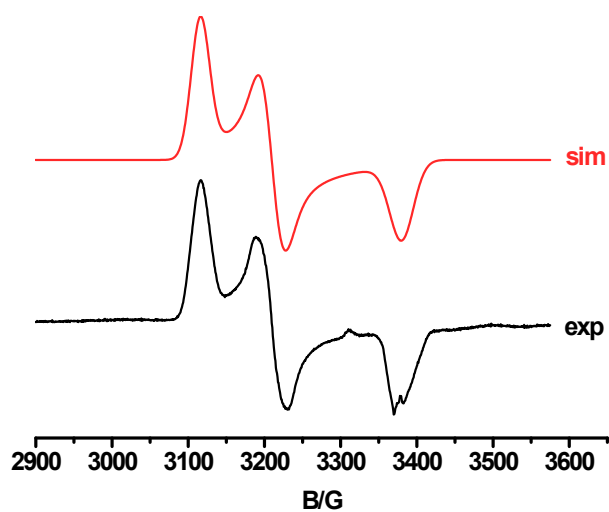


Figure S3. ESR Spectrum of the chemically reduced species 2^+ with Cp_2Co in toluene, 120 K

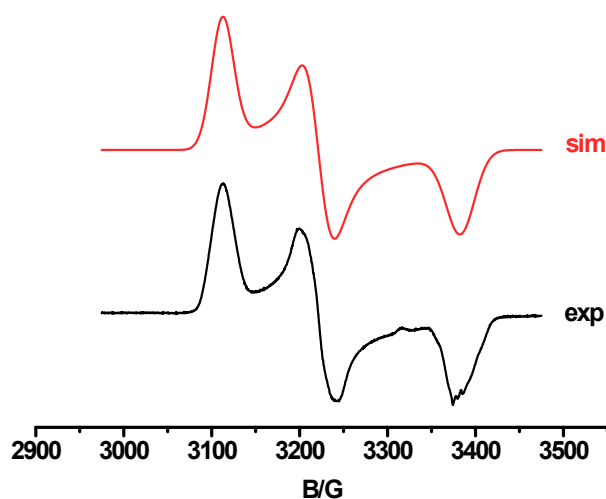


Figure S3. ESR Spectrum of the chemically reduced species 3^+ with Cp_2Co in toluene, 120 K

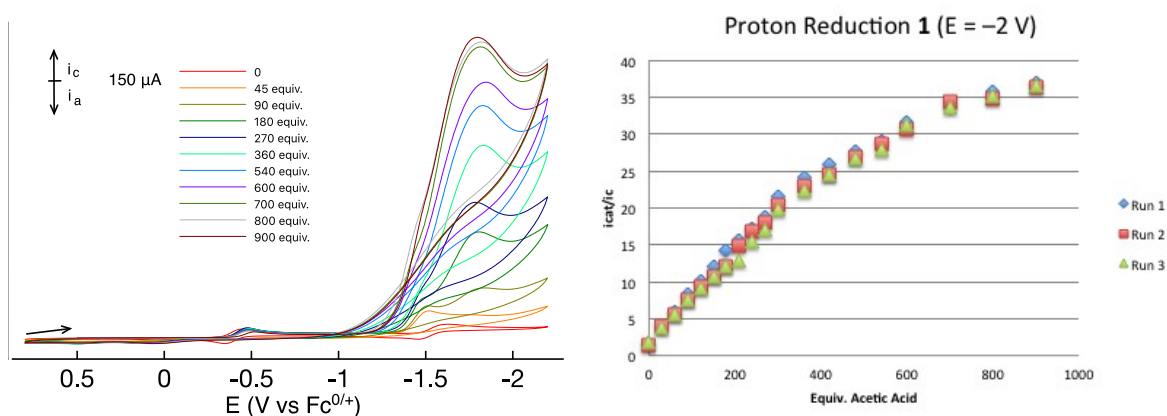


Figure S4. Electrocatalytic reduction of acetic acid by **1** in $\text{CH}_3\text{CN}/0.1 \text{ M Bu}_4\text{NPF}_6$ at 298 K, the scan rate was 100 mV/s with a 1 mm glassy carbon working electrode, Pt counter electrode, Ag reference electrode. Catalytic current (i_c) to the peak current of the Ni(II/I) couple in the absence of acid (i_p) as a function of the concentration of acetic acid. Select voltammograms displayed as example of a typical run, select plots are

displayed for clarity, full runs were performed at 30 equiv. of acetic acid intervals.

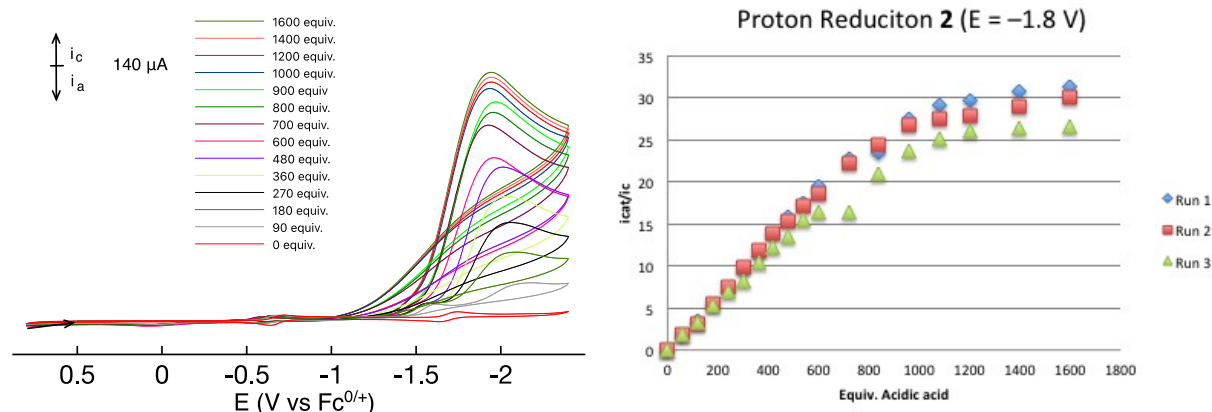


Figure S5. Electrocatalytic reduction of acetic acid by **2** in $\text{CH}_3\text{CN}/0.1 \text{ M Bu}_4\text{NPF}_6$ at 298 K, the scan rate 100 mV/s with a 1 mm glassy carbon working electrode, Pt counter electrode, Ag reference electrode. Catalytic current (i_c) to the peak current of the Ni(II/I) couple in the absence of acid (i_c) as a function of the concentration of acetic acid. Select voltammograms displayed as example of a typical run, select plots are displayed for clarity, full runs were performed at 30 equiv. of acetic acid intervals.

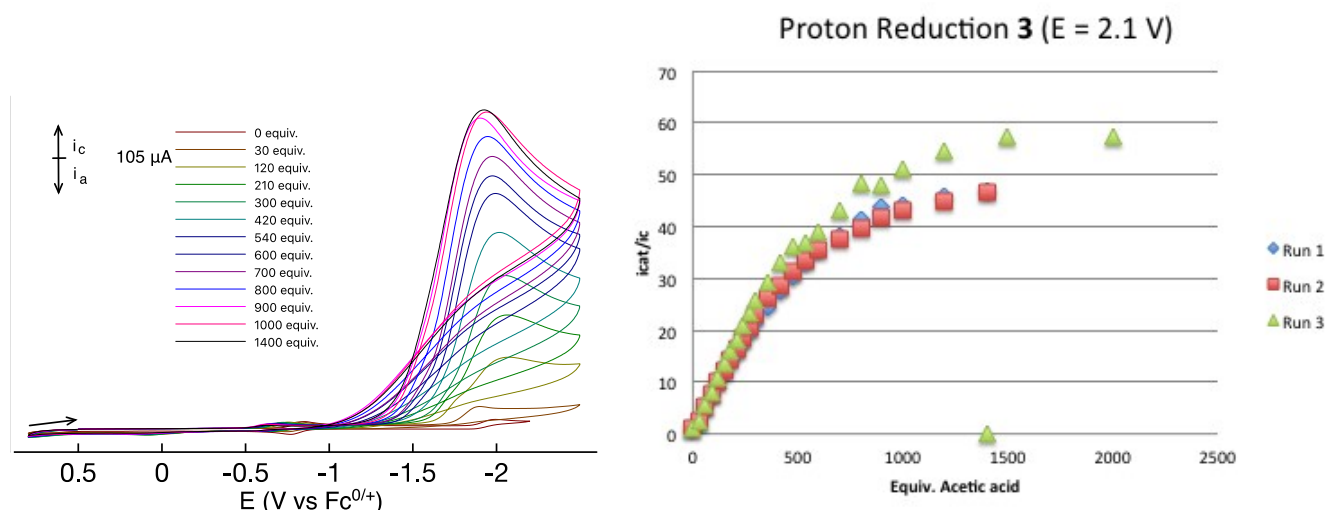


Figure S6. Electrocatalytic reduction of acetic acid by **3** in $\text{CH}_3\text{CN}/0.1 \text{ M Bu}_4\text{NPF}_6$ at 298 K, the scan rate was 100 mV/s with a 1 mm glassy carbon working electrode, Pt counter electrode, Ag reference electrode. Catalytic current (i_c) to the peak current of the Ni(II/I) couple in the absence of acid (i_c) as a function of the concentration of acetic acid. Select voltammograms displayed as example of a typical run, select plots are displayed for clarity, full runs were performed at 30 equiv. of acetic acid intervals.

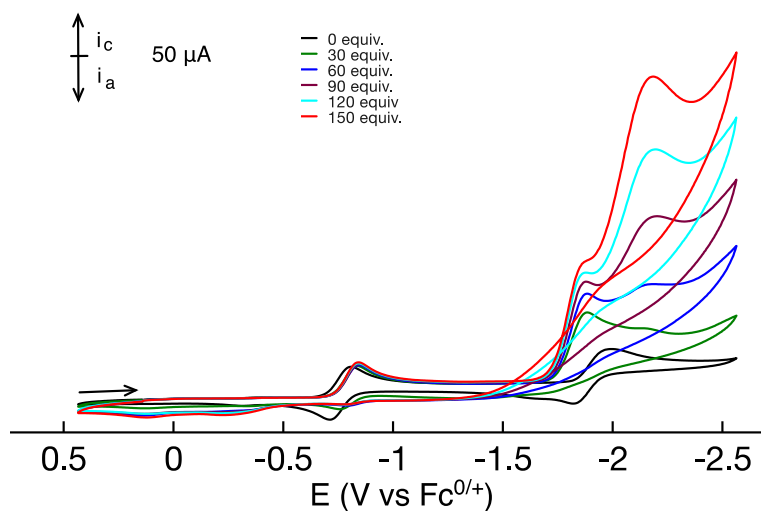


Figure S7. Electrocatalytic reduction of acetic acid at lower concentrations by **3** in $CH_3CN/0.1 M Bu_4NPF_6$ at 298 K, the scan rate was 100 mV/s with a 1 mm glassy carbon working electrode, Pt counter electrode, Ag reference electrode.

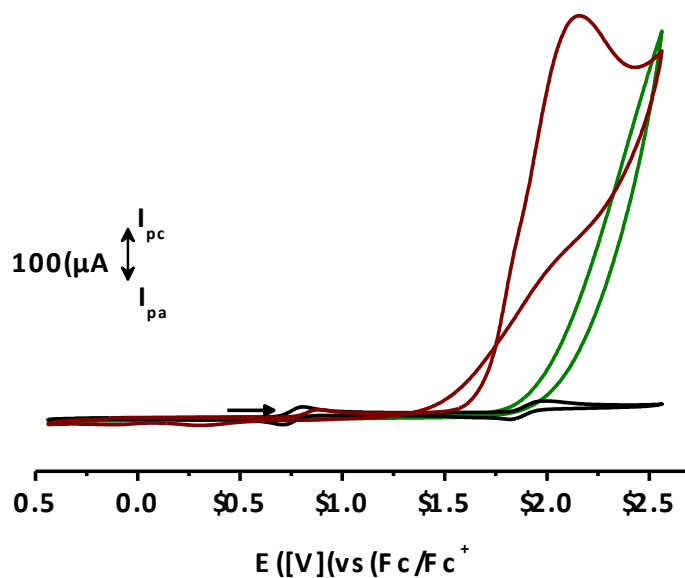


Figure S8. Cyclic voltammetry of acetic acid with **3** (red) and without **3** (green) in $CH_3CN/0.1 M Bu_4NPF_6$ at 298 K, the scan rate was 100 mV/s with a 1 mm glassy carbon working electrode, Pt counter electrode, Ag reference electrode.